J Pharm Anal Vol 1, No 1, 32 - 38 (2011)

ORIGINAL ARTICLES

Simultaneous determination of captopril and hydrochlorothiazide by time-resolved chemiluminescence with artificial neural network calibration

Han-Chun Yao[1], Min Sun[1], Xiao-Feng Yang[2], Zhen-Zhong Zhang[1], Hua Li[3]*

[1] *School of Pharmaceutical Science, Zhengzhou University, Zhengzhou 450001, China;* [2] *Department of Chemistry, Northwest University, Xi'an 710069, China;* [3] *Institute of Analytical Science, Northwest University, Xi'an 710069, China.*

Abstract: The combined use of chemometrics and chemiluminescence (CL) measurements, with the aid of the stopped-flow mixing technique, developed a simple time-resolved CL method for the simultaneous determination of captopril (CPL) and hydrochlorothiazide (HCT). The stopped-flow technique in a continuous-flow system was employed in this work in order to emphasize the kinetic differences between the two analytes in cerium (IV)-rhodamine 6G CL system. After the flow was stopped, an initial rise of CL signal was observed for HCT standards, while a direct decay of CL signal was obtained for CPL standards. The mixed CL signal was monitored and recorded on the whole process of continuous-flow/stopped-flow, and the obtained data were processed by the chemometric approach of artificial neural network. The relative prediction error (RPE) of CPL and HCT was 5.9% and 8.7%, respectively. The recoveries of CPL and HCT in tablets were found to fall in the range between 95% and 106%. The proposed method was successfully applied to the simultaneous determination of CPL and HCT in a compound pharmaceutical formulation.

Keywords: time-resolved chemiluminescence; artificial neural network; captopril; hydrochlorothiazide

1 Introduction

Chemiluminescence (CL) has been known as a powerful and important analytical technique because the analytical performance of CL detection is better than that of other common spectroscopic detection methods (such as spectrophotometry and fluorescence), with some advantages including low detection limits, wide linear ranges, high analytical frequency and simple instrumentation[1]. Liquid-phase CL reactions have been used for the sensitive, selective detection in a wide range of analytical techniques including flow injection analysis (FIA), sequential injection analysis (SIA), high performance liquid chromatography (HPLC) and capillary electrophoresis (CE). The primary field of application has so far been for process analysis, both off-line and on-line. Moreover, studies are under way for application to environmental, pharmaceutical and clinical analysis.

Time-resolved chemiluminescence is a kinetic-based CL method using the stopped-flow technique, with some advantages such as selectivity, sensitivity and less consumption of the reagents. As a novel detection mode, time-resolved CL has been used for the detection of naloxone [2], hydrochlorothiazide [3] and captopril [4], respectively. In the above-mentioned work, different CL systems were studied using the stopped-flow technique in a continuous-flow system. The mentioned method was based on the recording of the whole CL intensity-versus-time profile that enables the use of total area, CL formation rate and CL decay rate, which are proportional to the analyte concentration. Then, Murillo Pulgarín *et al.* [5] developed a time-resolved CL method for the simultaneous stopped-flow determination of morphine and naloxone using a two equation system. In addition, time-resolved electrochemiluminescence of platinum (II) coproporphyrin [6] and hot electron-induced time-resolved electrogenerated chemiluminescence of a europium (III) label in fully aqueous solutions [7] have also been reported.

Captopril (1-[(2S)-3-mercapto-2-methylpropionyl]-L-proline, CPL) is an orally active inhibitor of the angiotensin-converting enzyme and widely used for the treatment of hypertensive diseases on its own or in combination with other drugs [8]. Hydrochlorothiazide (6-chloro-3, 4-dihydro-1, 2, 4-benzothiadiazine-7-sulphonamide-1, 1-dioxide, HCT) is a popular thiazide diuretic that acts directly on the kidney by increasing the excretion of sodium chloride and water and, to a lesser extent, that of potassium ion as well [3]. In market, CPL is commercialized with HCT as it can improve the action of hypotensive substances allowing a decrease of the dose in order to prevent possible secondary effects. Quantitative analysis of the samples containing CPL and HCT has been reported by spectrophotometry [9,10] and HPLC [11,12]. However, UV derivative spectrophotometry involves some complicated procedures and is time-consuming. Ouyang *et al.* [11] reported the determination of CPL and HCT by narrow-bore liquid chromatography combined with CL detection. Subsequently,

Received 31 May 2010; Accepted 1 August 2010

* Corresponding author. E-mail: huali@nwu.edu.cn

a pre-column UV derivatization procedure combined with HPLC separation is proposed for the determination of CPL together with HCT in human plasma [12]. However, these reported methods suffered from disadvantages such as complicated procedure, long response time and requirement of expensive instruments.

The CL detection technique has been successfully developed for the determination of CPL [4,13,14] and HCT [3, 15,16], respectively. Zhang *et al.* [13] proposed a flow injection CL analytical method for the determination of CPL. The method was based on the CL reaction of CPL with cerium (Ⅳ) in sulphuric acid, and sensitized by rhodamine 6G. Later, this same system was also applied for the determination of HCT [15]. Therefore, the proposed CL method cannot be used for analysis of samples containing both CPL and HCT due to the lack of selectivity. Recently, a time-resolved CL was developed for the determination of HCT and CPL respectively [3, 4]. Although there are no mutual interferences on individual determination, its analytical usefulness for the simultaneous determination of CPL and HCT based on their different kinetic behaviors, has never been demonstrated to date.

In recent years, multivariate calibration methods, such as classical least squares (CLS), principal component regression (PCR), partial least squares (PLS) and artificial neural network (ANN), have been applied to the handling of the analytical data obtained in all the instrumentations [17-19]. Several multivariate calibration methods applied to the CL analysis have been reported, including PLS [20-22], ANN [23,24] and kalman filter [25]. ANN based on artificial intelligence is powerful non-parametric non-linear modeling techniques [26-28]. Li *et al.* [23] proposed a continuous-flow CL system with back propagation (BP)-ANN calibration for the simultaneous determination of rifampicin and isoniazid. Shen *et al.* [24] reported a method of simultaneous determination of iron (Ⅱ) and antimony (Ⅲ) with ANN combined with flow injection-induced kinetics using liquid CL. In their work, the CL intensity was measured and recorded in a flow system to indirectly show the kinetic properties of analytes. Kinetic methods based on the stopped-flow mixing approach are gaining interest in chemical analysis due to the ease of automation of the instrument operation and data handling. The stopped-flow mixing technique is a very appropriate approach for achieving the reproducible mixing of sample and reagents in CL studies. In addition, coupling a data acquisition unit permits the complete CL intensity-time profile to be obtained easily [29].

In this paper, a simple time-resolved CL method combined with ANN calibration for the simultaneous determination of CPL and HCT was proposed. The method was based on the different kinetic behaviors of the two analytes in cerium (Ⅳ)-rhodamine 6G CL reaction using the stopped-flow technique in a continuous-flow system. Stopped-flow technique was employed in this work in order to emphasize kinetic differences and obtain complete response curves. The CL intensity was measured and recorded every tenth second during the whole process and all the data were processed by ANN calibration. The proposed method was successfully applied to the simultaneous determination of CPL and HCT in pharmaceutical preparations.

2 Theoretical background

In this work, the kinetic data obtained from experiments were processed by ANN, which was trained with the back-propagation of errors learning algorithm. Its basic theory and application to chemical problems can be found in the literature [30]. The neural network performs a non-linear iterative fit of data. The structure of the network comprises three node layers: an input layer, a hidden layer and an output layer. The nodes in the input layer transfer the input data to all nodes in the hidden layer. These nodes calculate a weighted sum of the inputs that is subsequently subjected to a non-linear transformation

$$O_j = f\left(\sum_{i=1}^{l} S_i \omega_{ij}\right) \quad (1)$$

where S_i is the input to the node i in the input layer, l is the number of nodes in the input layer, ω_{ij} (weights) are the connections between each node i in the input layer and each node j in the hidden layer, O_j is the output of node j in the hidden layer, and f is a non-linear function.

The output of the network is a weighted sum of the outputs of the hidden layer and it is considered as the calculated concentration. During the training process (i.e. calibration) the weights are iteratively calculated in order to minimize the sum of squared difference between the known concentrations and the calculated concentrations. The correction of weights $\Delta\omega_{ij}$ was defined as follows:

$$\Delta\omega_{ij(n+1)} = \eta\delta_j O_j + \alpha\Delta\omega_{ij(n)} \quad (2)$$

where δ_j is the error term, η is the learning rate, α is the momentum and n is the iteration number. The iteration would be finished when the error of prediction reached a minimum.

Principal components analysis (PCA)-ANN is an improved ANN model, which has been applied widely [30]. In this work, PCA was applied in the form of data pretreatment of the calibration data matrix of CPL and HCT mixtures, and the PC scores were then used as the input of the network. When the PCA data reduction procedure is applied prior to the construction of the non-linear ANN model, its dimensional effect is to increase the numerical stability of the model construction process and reduce the amount of colinearity between variables. In this study, PCA-ANN architectures were constructed using different number of PCs with one bias node for the input layer. The multilayer feed forward PCA-ANN was trained by the BP algorithm, and the variables of PCA-ANN architecture were optimized to obtain the minimum error of the prediction set.

For the optimized model, two parameters were selected to test the prediction ability of the BP-ANN models for each component: the root mean square difference (RMSD) and the relative prediction error (RPE), which can be calculated for each component as follows:

$$\mathrm{RMSD} = \sqrt{\frac{\sum_{i=1}^{n} (\hat{y}_i - y_i)^2}{n}} \quad (3)$$

$$\mathrm{RPE} = \sqrt{\frac{\sum_{i=1}^{n} (\hat{y}_i - y_i)^2}{\sum_{i=1}^{n} \hat{y}_i^2}} \times 100\% \quad (4)$$

where $\hat{y}_i$ is the true concentration of the analyte in the sample i, y_i represents the estimated concentration, and n is the total number of samples used in the prediction set.

3 Experimental

3.1 Apparatus and software

The flow system was installed in a conventional manifold as shown in Figure 1. The reaction reagents [sample solution, rhodamine 6G and Ce (IV) solutions] were pumped through the three-line manifold by a peristaltic pump (IFIS-C, Xi'an Ruike Electronic Science-Tech. Co., Ltd., China) with a flow rate of 1.0 mL/min. The reagents went through PTFE flow tubes (Tygon, 0.8 mm i.d.), were carried to the flow cell (a planar coiled colorless glass tubing, 100 mm × 2 mm i.d), and positioned in front of the detection window of the photomultiplier tube (PMT). The CL signal produced in the flow cell was collected with a CR-150 PMT (operated at −600V, Hamamatsu, Tokyo, Japan) of BPCL ultra-weak luminescence analyzer (Institute of Biophysics, Academia Sinica, Beijing, China). After the CL signal reached the plateau, the flow was stopped and the dynamic process of CL can be monitored on line with CL kinetic curves. The signal was recorded using a compatible computer equipped with a data acquisition interface. Data acquisition and treatment were performed with BPCL software running under Windows 98.

The data pretreatment was done with MATLAB 6.5. The calculations of ANN and the performance of PCA input selections were carried out using Trajan software version 3.0 (Durham, UK) on a Pentium IV personal computer.

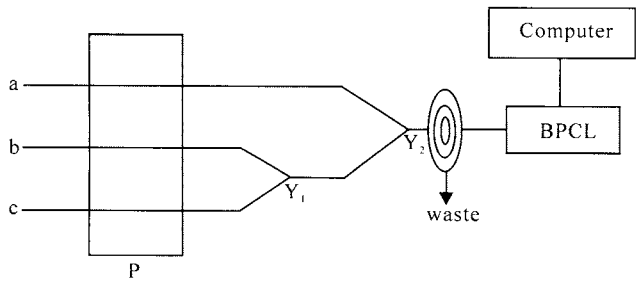

Figure 1 Schematic diagram of the stopped-flow CL system used for the determination of CPL and HCT. a, Ce(IV); b, sample solution; c, rhodamine 6G; P, peristaltic pump; Y_1, Y_2, three-way junction; F, CL flow cell; BPCL, BPCL ultra-weak luminescence analyzer.

3.2 Reagents and solutions

All the reagents were of analytical grade and all solutions were prepared in doubly distilled water. 8.0 mM Ce (IV) solution (Hunan Institute for Non-ferrous Geology Research) was prepared with 0.1 M sulfuric acid solution daily. A stock solution of 1.0 mM rhodamine 6G (Sigma) was prepared by dissolving 0.0479 g rhodamine 6G in 100 mL water. A standard solution of 0.1 mg/mL hydrochlorothiazide (HCT, Institute of Shaanxi Pharmaceutical Industry, China) was prepared with basic medium and diluted with water to prepare working solutions. Standard solution of 0.1 mg/mL captopril (CPL, Changzhou Pharmaceutical Factory Co., Ltd., China) was prepared by dissolving 10 mg of captopril in water and diluting to 100 mL. Working standard solutions were then prepared by appropriate dilution of this standard solution. Stock solutions of CPL and HCT were stored at the room temperature and protected from the light. Stock solution of 2.0 M H_2SO_4 was also prepared.

3.3 Procedures for stopped-flow analysis in a continuous-flow system

The continuous-flow manifold used to implement the stopped-flow system is depicted schematically in Figure 1. The sample and rhodamine 6 G solutions were first mixed at Y_1 and merged with Ce (IV) solution stream at Y_2, and then reached the mixing coil, producing the CL signal. The pumping was continued until a stable CL signal was recorded, and then the reagent streams were stopped by turning off the pump for 60 s. In this way, the transient CL signal was continuously monitored to obtain a plot of CL intensity versus time. After measurement, sample solution was washed with the water stream and the CL signal returned to the baseline (produced by the oxidation of rhodamine 6 G) for the next measurement. Finally, the pump was restarted to operate for at least 30 s. After the CL signal reached the plateau, the flow was stopped again.

4 Results and discussion

4.1 Kinetic profiles of CPL and HCT in present CL system

Before carrying out the stopped-flow method, the batch method for the CL profiles was applied. For the oxidation reaction between Ce (IV) and rhodamine 6G, a weak light emission was obtained. After adding CPL or HCT into the above mixing solution, an enhancive CL emission was observed. As shown in Figure 2, the CL reaction of Ce (IV)-rhodamine 6G-CPL was a rapid-type luminescent one, and the time interval between the start of CL and its maximum was about 5.0 s before the CL intensity gradually decreased to the baseline after 25 s (Figure 2a). However, the CL emission of Ce (IV)-rhodamine 6G-HCT system was slow and long-lived, and the CL intensity increased slowly and reached a plateau in the range of 10 − 40 s before it gradually decreased with the increase of time (Figure 2b). Thus, the kinetic properties of CPL and HCT were

obviously different in the static system.

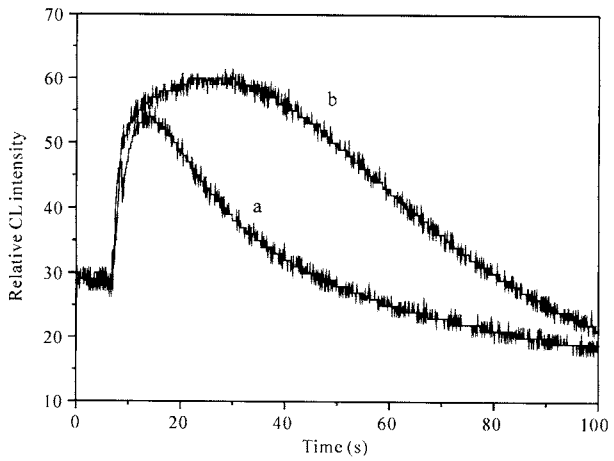

Figure 2 CL-time profiles in the static system. a, 1.0 mL of 1.0 μg/mL CPL + 1.0 mL of the mixture of rhodamine 6G (5.0 μM) and Ce (IV) (8.0 mM in 0.2 M H_2SO_4). b, 1.0 mL of 1.0 μg/mL HCT + 1.0 mL of the mixture of rhodamine 6G (5.0 μM) and Ce(IV) (8.0 mM in 0.2 M H_2SO_4). The high voltage was set at −600V.

4.2 CL-time profiles of CPL and HCT in stopped-flow system

In this work, the stopped-flow technique in a continuous-flow system was used to emphasize the different kinetic behaviors between CPL and HCT. The continuous-flow/stopped-flow allowed the simple extraction of kinetics information with little influence of dispersion-affected variables. The CL registers from Ce (IV)-rhodamine 6G-CPL/HCT reaction were obtained according to stopped-flow theoretical background. The time-intensity register was composed of two regions according to the point where the continuous flow was stopped. Previous to maximum intensity, the register was obtained from a system of continuous sample injection. The response was only the chemical process of formation of a chemical species. After the CL intensity achieved a plateau, the flow was stopped and the register was obtained from a stopped-flow system. In this region, the difference of kinetic characteristic between CPL and HCT was displayed by the CL-time profiles (Figure 3).

In Figure 3, the examples of stopped-flow registers for standard solutions of CPL and HCT and for a mixed sample are shown. From Figure 3a, it can be seen that CL intensity for CPL standard decayed after the flow was stopped, which is the result of consuming of CL species. Figure 3b shows the CL register obtained for HCT standard. The CL intensity continually increased and reached its maximum value, and then gradually decreased with the increase of time. This profile indicated that the CL emission of HCT was long-lived and the light-emitting products were still generated after the flow was stopped. A comparison between Figure 3a and 3b showed that both the luminescence lifetime and the CL intensity of HCT were stronger than those of CPL. Finally, as can be seen from Figure 3c, the CL register obtained for the mixed solution of CPL and HCT had an intermediate rise. The CL intensity of the mixed solution increased in the continuous-flow system; however, after the flow was stopped, the maximum value of CL intensity decreased sharply compared with that of Figure 3b. It is evidently shown that there is an interaction between CPL and HCT and the present system is nonlinear. ANN calibration can model the nonlinear system with no prior knowledge of the system and eliminate or reduce the effects of analyte interactions. This ability makes it particularly attractive for calibration in kinetic mixture resolution. Thus, in this paper, we employed ANN algorithms combined with PCA input selection to model a function and predict the concentrations of samples.

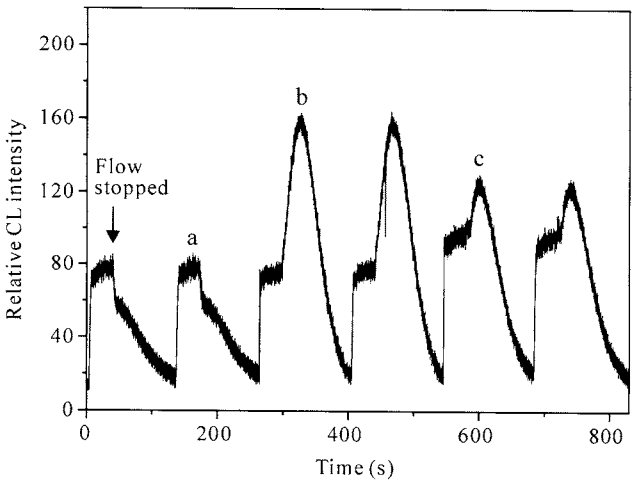

Figure 3 Time-resolved CL analysis plot of repeated injection of samples. a, 1.0 μg/mL CPL; b, 0.5 μg/mL HCT; c, the mixture of CPL and HCT.

4.3 Optimization of experimental conditions

2.0×10^{-6} g/mL CPL and 1.0×10^{-6} g/mL HCT solutions were used to optimize the experimental conditions using the stopped-flow technique in a continuous-flow system. The parameters optimized included the concentrations of the reagents used for the CL reaction and the flow rate.

For the Ce (IV), the concentration range of 1.0 − 10.0 mM was tested. As the concentration of Ce (IV) increased, the CL signal of both CPL and HCT increased. The CL signal-to-noise ratio (S/N) reached maximum when 8.0 mM Ce (IV) was used. Thus, 8.0 mM Ce (IV) was selected for subsequent experiments. Ce (IV) reacts with rhodamine 6G and HCT/CPL to produce light emission in acidic solution. The nature and concentration of the acid used in the reaction were tested in order to obtain the optimal conditions. H_2SO_4 produced the strongest CL signal and was selected as an acidic medium. The maximum CL intensity was obtained when the H_2SO_4 concentration was between 0.15 M and 0.25 M, and then CL intensity decreased with the increase of H_2SO_4 concentration. Thus, 0.2 M H_2SO_4 was chosen for further experiment.

The effect of rhodamine 6G concentration on the CL intensity was investigated in the range of $2.0\times10^{-5}-2.0\times10^{-4}$ M. As can be seen from Figure 4a, the CL intensity for HCT increased gradually with the increase of concen-

tration of rhodamine 6G, and reached a plateau in the range of 5.0×10^{-5} – 1.0×10^{-4} M. However, Figure 4b shows that the CL intensity for CPL decreased rapidly with the increase of the concentration of rhodamine 6G up to 8.0×10^{-5} M, above which the CL signal descended only slowly. As a compromise of high sensitivity for CPL and HCT, the concentration of rhodamine 6G was chosen at 5.0×10^{-5} M.

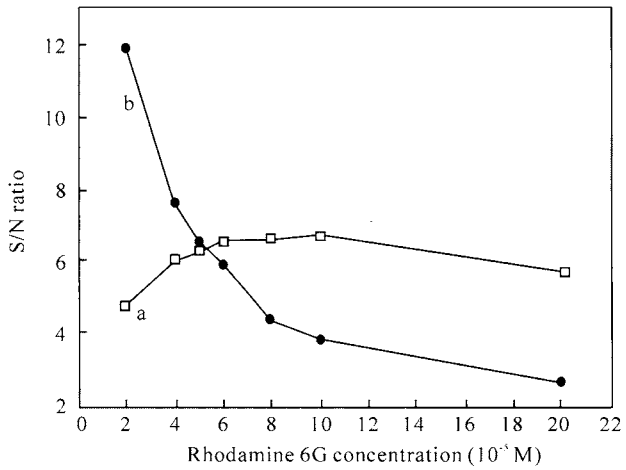

Figure 4 Effect of rhodamine 6G concentration on the CL intensity. a, HCT 0.5 μg/mL; b, CPL 1.0 μg/mL. Ce(IV), 8.0 mM; H_2SO_4, 0.2 M.

The flow rate of the solutions is very important to the CL detection because the time taken to transfer the excited product into the flow cell is critical for maximum collection of the emitted light. The effect of flow rate on the kinetic curve was studied over the range of 1.0 – 3.0 mL/min under the above selected conditions and it was found that the signal-to-noise ratio almost remained constant with increasing flow rate. As a compromise between CL intensity and background noise, a flow rate of 1.0 mL/min was recommended.

4.4 Univariate calibration

Under the optimum conditions described above, the calibration graph of emission intensity versus CPL concentration was linear in the range 0.2 – 4.0 μg/mL and the detection limit was 0.08 μg/mL (3σ). The calibration graph of emission intensity versus HCT concentration was linear in the range 0.1 – 6.0 μg/mL and the detection limit was 0.03 μg/mL (3σ). The relative standard deviations ($n=9$) were 2.9% for 1.0 μg/mL CPL and 2.1% for 1.0 μg/mL HCT, respectively.

4.5 Multivariate calibration

In this experiment, calibration data matrix of CPL and HCT mixtures was established according to the principle of orthogonal design (5^2). The concentration data of the standards are listed in Table 1. In order to avoid "over training", the data set consisting of 25 standard solutions with different concentrations of CPL and HCT was divided into the training set and test set at random. Thus weights are calculated from a training set while the concentration of the test set is being simultaneously predicted. To evaluate the prediction ability of ANN model, a set of 6 synthetic verification mixtures containing the two analytes were prepared. All the data were mean centered before PCA procedure and ANN training.

Table 1 Concentration data for different mixtures used for calibration of captopril (CPL) and hydrochlorothiazide (HCT)

Mixture	CPL ($\times10^{-6}$ g/mL)	HCT ($\times10^{-6}$ g/mL)
1	0.5	0.3
2	0.5	0.9
3	0.5	1.5
4	0.5	3.0
5	0.5	6.0
6	1.0	0.3
7	1.0	0.9
8	1.0	1.5
9	1.0	3.0
10	1.0	6.0
11	1.5	0.3
12	1.5	0.9
13	1.5	1.5
14	1.5	3.0
15	1.5	6.0
16	2.5	0.3
17	2.5	0.9
18	2.5	1.5
19	2.5	3.0
20	2.5	6.0
21	5.0	0.3
22	5.0	0.9
23	5.0	1.5
24	5.0	3.0
25	5.0	6.0

In this section, CL kinetic data from the beginning of the stopped-flow up to 60 s were chosen for the calculations, which contained 600 points that were collected every tenth second. When no PCA procedure was performed, 600 data had to be used as input variables of ANN. Therefore, PCA of the kinetic data of the calibration mixtures was previously performed and the scores of this model were used as input data to the network. This reduces the ANN-training time substantially without losing information. In this analysis, the number of principal components to be included in the PCA-ANN model was investigated and the optimum number of PCs was obtained. The RPE obtained with the number of PCs was plotted (Figure 5), and from these graphs it is clear that the RPE for each analyte reached a minimum at six PCs for both analytes, and thus six were selected for modeling. All parameters for the network models were tested, and those chosen for inclusion in the analytical model corresponded to the minimum value of the RPE.

Error back-propagation (BP) network is one of the most widely used ANN in solving the problem of regression or classification. Therefore, in this paper, the application of BP-ANN for the determination of binary mixtures was studied. The PCA process of the data set gave six important principal components, which represented nearly 100% of the variability in the data set. Therefore, the six principal

components were applied as the corrected input variables to the corresponding BP-ANN model instead of the original data. When the six principal components were investigated, the Trajan automatic network designer designed a 6 : 4 : 2 BP-ANN in 1000 iteration times with unit penalty 0.01. After the models were established and trained respectively, we use the models to predict 6 synthetic mixtures. All the calculated results in this section are listed in Table 2. From the calculated results, it is shown that PCA-ANN is a more effective calibration method with better prediction (lower RPEs). The PCA-ANN modeling simplified the training procedure of the ANN; the inclusion of only the significant PCs in the model decreased the contribution of experimental noise and other minor extraneous factors.

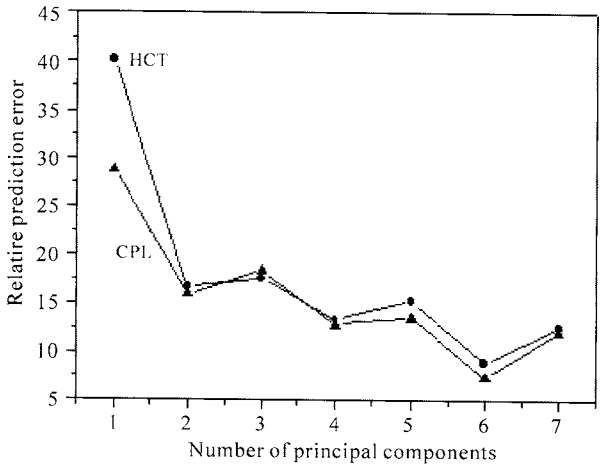

Figure 5 Plot of RPE of binary mixtures *vs.* the number of principal components used in PCA-ANN

Table 2 Prediction results for synthetic mixtures of CPL and HCT

Synthetic mixture	CPL ($\times 10^{-6}$ g/mL)		HCT ($\times 10^{-6}$ g/mL)	
	Added	Found	Added	Found
No.1	1.0	1.04	0.6	0.67
No.2	1.0	1.07	1.0	0.94
No.3	1.0	1.16	1.2	1.12
No.4	1.6	1.51	1.0	0.90
No.5	1.6	1.60	0.6	0.69
No.6	2.0	1.95	0.6	0.57
RMSD		0.08		0.07
RPE		5.88		8.68

4.6 Interference study

Some common ions and excipients in the pharmaceutical product were investigated to test their influence on the determination of the two analytes by the proposed method. The effect was examined by analyzing a standard mixture solution of 1.0 μg/mL HCT and 1.6 μg/mL CPL to which increasing amounts of interfering species were added. The tolerable concentration ratios for interference at the 5% level were over 1 000 for Na^+, Mg^{2+}, Ba^{2+}, K^+, Cl^-, SO_4^{2-}, and NO_3^-; 500 for starch, dextrin, glucose, sucrose and lactose; 100 for fructose and EDTA; and 10 for ascorbic acid. These results indicate that some common ions and excipients hardly have effect on the determination of CPL and HCT. Thus, the selectivity for the proposed method is satisfactory and the present method may be directly applied to the determination of CPL and HCT in pharmaceutical preparations.

4.7 Application to analysis of tablets

The proposed method was also successfully applied to the determination of CPL and HCT in two commercial tablets according to the procedures described by Murillo Pulgarín *et al* [3]. The analytical results obtained by PCA-ANN, and the recovery results by the standard addition are summarized in Table 3, which agree well with the manufacturers' stated contents. The results show that the prediction ability of the proposed PCA-ANN model for the two analytes in real samples is satisfactory.

5 Conclusion

In this paper, a simple time-resolved CL system combined with artificial neural network calibration was successfully applied to the simultaneous determination of CPL and HCT in compound formulations without prior separation. The present results demonstrate that the coupling of the stopped-flow mixing technique and the CL reaction of CPL or HCT with cerium (IV) and rhodamine 6G is a very suitable approach for the extraction of kinetics information and obtaining complete response curves. Compared with reported methods (HPLC and UV), this method has the potential advantages of simple apparatus, convenient operation, high sensitivity and less reagent consumption. Further studies are being carried out to expand its application for the simultaneous determination of multicomponent substances in the complex system.

Table 3 Determination of CPL and HCT in tablets by PCA-ANN method

Sample	Labeled value (mg)		Proposed method (mg)		Added($\times 10^{-6}$ g/mL)		Recovered ($\times 10^{-6}$ g/mL)		Recovery (%)	
	CPL	HCT	CPL	HCT	CPL	HCT	CPL	HCT	CPL	HCT
No.1	10.0	6.0	9.89	6.17	0.50	0.30	0.49	0.29	98	97
					1.00	0.60	0.96	0.59	96	98
No.2	10.0	6.0	10.35	6.34	0.50	0.30	0.53	0.31	106	103
					1.00	0.90	0.95	0.87	95	97

Acknowledgments

This work was supported by the National Natural Science Foundation of China (No.20675063).

References

[1] Li BX, Zhang ZJ, Jin Y. Plant tissue-based chemiluminescence flow biosensor for glycolic acid. *Anal Chem*, 2001, 73(6):1203-1206.

[2] Murillo Pulgarín JA, García Bermejo LF, Rubio Aranda JA. Time-resolved chemiluminescence: a novel tool for improved emission sequence in stopped-flow analysis:Application to a kinetic study of the oxidation of naloxone. *Anal Chim Acta*, 2004, 517(1-2):111-117.

[3] Murillo Pulgarín JA, Alañón Molina A, Pérez-Olivares Nieto G. Determination of hydrochlorothiazide in pharmaceutical preparations by time resolved chemiluminescence. *Anal Chim Acta*, 2004, 518(1-2):37-43.

[4] Murillo Pulgarín JA, García Bermejo LF, Fernández López Pablo. Sensitive determination of captopril by time-resolved chemiluminescence using the stopped-flow analysis based on potassium permanganate oxidation. *Anal Chim Acta*, 2005, 546(1):60-67.

[5] Murillo Pulgarín JA, García Bermejo LF, Lemus Gallego JM, *et al.* Simultaneous stopped-flow determination of morphine and naloxone by time-resolved chemiluminescence. *Talanta*, 2008, 74(5):1539-1546.

[6] Canty P, Väre L, Håkansson M, *et al.* Time-resolved electrochemiluminescence of platinum(II) coproporphyrin. *Anal Chim Acta*, 2002, 453 (2):269-279.

[7] Jiang Q, Håkansson M, Spehar AM, *et al.* Hot electron-induced time-resolved electrogenerated chemiluminescence of a europium(III) label in fully aqueous solutions. *Anal Chim Acta*, 2006, 558(1-2):302-309.

[8] Rahman N, Singh M, Hoda N. Validation of simultaneous volumetric and spectrophotometric methods for the determination of captopril in pharmaceutical formulations. *Farmaco*, 2005, 60(6-7):569-574.

[9] Tomšů D, Catalá Icardo M, Martínez Calatayud J. Automated simultaneous triple dissolution profiles of two drugs, sulphamethoxazole-trimethoprim and hydrochlorothiazide-captopril in solid oral dosage forms by a multicommutation flow-assembly and derivative spectrophotometry. *J Pharm Biomed Anal*, 2004, 36(3):549-557.

[10] Panderi I, Parissi-Poulou M. Determination of captopril and captopril-hydrochlorothiazide combination in tablets by derivative UV spectrophotometry. *Int J Pharm*, 1992, 86(2-3):99-106.

[11] Ouyang J, Baeyens WRG, Delanghe J, *et al.* Chemiluminescence-based liquid-chromatographic determination of hydrochlorothiazide and captopril. *Anal Chim Acta*, 1999, 386(3):257-264.

[12] Huang TM, He Z, Yang B, *et al.* Simultaneous determination of captopril and hydrochlorothiazide in human plasma by reverse-phase HPLC from linear gradient elution. *J Pharm Biomed Anal*, 2006, 41(2):644-648.

[13] Zhang ZD, Baeyens WRG, Zhang XR, *et al.* Chemiluminescence flow-injection analysis of captopril applying a sensitized rhodamine 6G method. *J Pharm Biomed Anal*, 1996, 14(8-10):939-945.

[14] Economou A, Themelis DG, Theodoridis G, *et al.* Sensitive determination of captopril by flow injection analysis with chemiluminescence detection based on the enhancement of the luminol reaction. *Anal Chim Acta*, 2002, 463(2):249-255.

[15] Ouyang J, Baeyens WRG, Delanghe J, *et al.* Cerium (IV)-based chemiluminescence analysis of hydrochlorothiazide. *Talanta*, 1998, 46(5):961-968.

[16] Xi J, Ji XH, Zhang SH, *et al.* Investigation of RuBPS-Ce(IV) chemiluminescence reaction and its application in determination of two diuretics. *Anal Chim Acta*, 2005, 541(1-2):191-196.

[17] Escandar GM, Damiani PC, Goicoechea HC, *et al.* A review of multivariate calibration methods applied to biomedical analysis. *Microchem J*, 2006, 82(1):29-42.

[18] Lozano VA, Camiña JM, Boeris MS, *et al.* Simultaneous determination of sorbic and benzoic acids in commercial juices using the PLS-2 multivariate calibration method and validation by high performance liquid chromatography. *Talanta*, 2007, 73(2):282-286.

[19] Ribeiro MPA, Pádua TF, Leite OD, *et al.* Multivariate calibration methods applied to the monitoring of the enzymatic synthesis of amipicilin. *Chemom Intell Lab Syst*, 2008, 90(2):169-177.

[20] Li BX, Wang DM, Lv JG, *et al.* Flow-injection chemiluminescence simultaneous determination of cobalt(II) and copper(II) using partial least squares calibration. *Talanta*, 2006, 69(1):160-165.

[21] Li BX, Wang DM, Lü JG, *et al.* Chemometrics-assisted simultaneous determination of cobalt(II) and chromium(III) with flow-injection chemiluminescence method. *Spectrochim Acta A*, 2006, 65(1):67-72.

[22] Murillo Pulgarín JA, García Bermejo LF, Nieves Sánchez García M. Multivariate calibration applied to the time-resolved chemilumnescence for the simultaneous determination of morphine and its antagonist naloxone. *Anal Chim Acta*, 2007, 602(1):66-74.

[23] Li BX, He YZ, Lü JG, *et al.* Simultaneous determination of rifampicin and isoniazid by continuous-flow chemiluminescence with artificial neural network calibration. *Anal Bioanal Chem*, 2005, 383(5):817-824.

[24] Shen JS, Zhang XS, Li SW, *et al.* Simultaneous determination of iron (II) and antimony(III) with an artificial neural network using liquid chemiluminescence. *Am Lab*, 2003, 35(4):14-15.

[25] Wang HX, Li JF, Chen ZX, *et al.* Fast simultaneous determination of niobium and tantalum by kalman filter analysis with flow injection chemiluminescence method. *Anal Sci*, 2005, 21(9):1051-1055.

[26] Ensafi AA, Khayanmian T, Benvidi A, *et al.* Simultaneous determination of copper, lead and cadmium by cathodic adsorptive stripping voltammetry using artificial neural network. *Anal Chim Acta*, 2006, 561(1-2):225-232.

[27] Ni YN, Zhang GW, Kokot S. Simultaneous spectrophotometric determination of maltol, ethyl maltol, vanillin and ethyl vanillin in foods by multivariate calibration and artificial neural networks. *Food Chem*, 2005, 89 (3):465-473.

[28] Chen YQ, Ni YN. Simultaneous spectrophotometric determination of four preservatives in foodstuffs by multivariate calibration and artificial neural networks. *Chin Chem Lett*, 2009, 20(5):615-619.

[29] Pérez-Ruiz T, Martínez-Lozano C, Tomás V, *et al.* Chemiluminescence determination of citrate and pyruvate and their mixtures by the stopped-flow mixing technique. *Anal Chim Acta*, 2003, 485(1):63-72.

[30] Zhang YX, Li H, Havel J. Modeling of the relationship between electroosmotic flow and separation parameters in capillary zone electrophoresis using artificial neural networks and experimental design. *Talanta*, 2005, 65(4):853-860.